

Characteristics of Internal Transport Barrier in JT-60U Reversed Shear Plasmas

Y. Sakamoto, Y. Kamada, S. Ide, T. Fujita, H. Shirai, T. Takizuka, Y. Koide, T. Fukuda,
T. Oikawa, T. Suzuki, K. Shinohara, R. Yoshino and the JT-60 Team

Naka Fusion Research Establishment, Japan Atomic Energy Research Institute,
Naka-machi, Naka-gun, Ibaraki-ken, 311-0193, Japan

e-mail contact of main author: sakamoty@fusion.naka.jaeri.go.jp

Abstract. Characteristics of internal transport barrier (ITB) structure are studied and the active ITB control has been developed in JT-60U reversed shear plasmas. The following results are found. Outward propagation of the ITB with steep T_i gradient is limited to the minimum safety factor location (ρ_{qmin}). However the ITB with reduced T_i gradient can move to the outside of ρ_{qmin} . Lower boundary of ITB width is proportional to the ion poloidal gyroradius at the ITB center. Furthermore the demonstration of the active control of the ITB strength based on the modification of the radial electric field shear profile is successfully performed by the toroidal momentum injection in different directions or the increase of heating power by neutral beams.

1. Introduction

One of the recent progresses in toroidal plasma research is characterized by formation of transport barriers in the core and the edge regions. Spontaneous transitions to improved confinement mode were first observed in the plasma edge with sufficient heating power [1]. The edge transport barriers (ETBs) formed the edge pedestals in the density and temperature profiles, where the local heat and particle transports were reduced. Recently spontaneous confinement bifurcations in the core region were observed in number of devices. In JT-60U, it was shown for the first time that the ITB appeared inside the region with the weak magnetic shear in high- β_p plasma [2], where the ion thermal diffusivity was decreased significantly. Clear reductions of the electron thermal diffusivity as well as the ion thermal diffusivity were found in the reversed magnetic shear plasmas [3,4] and the weak magnetic shear plasmas with high triangularity configuration [5]. These plasmas with improved confinement in the core region are compatible with a steady state operation based on bootstrap current [6], and the transport barrier for the electron temperature is desirable for the burning plasmas where the electron heating by the alpha particles is dominant.

It is important to understand the characteristics of the ITB because the plasmas with the ITB have high confinement properties and are compatible with non-inductive current drive, and therefore are a leading scenario of steady state operation for ITER. The high particle confinement, however, leads to helium ash accumulation and the steep pressure gradient under the large alpha heating power is unfavorable. Thus the active control of the ITB strength is indispensable toward the steady state operation. Several theoretical models for transport barrier formation suggest that the ExB flow shear plays an important role in suppressing the level of the turbulence and reducing the correlation length of the turbulence [7]. Therefore there is a possibility that the ITB can be controlled by the modification of the radial electric field profile.

This paper is organized as follows. Characteristics of ITB structure in JT-60U reversed shear plasmas are described in Sec. 2. Demonstrations of the active control of the ITB strength performed by the toroidal momentum injection in the different directions or the increase of heating power are described in Sec. 3. The conclusion is presented in Sec. 4.

2. Structures of Internal Transport Barrier

In JT-60U reversed shear plasmas, thermal and particle diffusivities decreased to the level of neoclassical value within the narrow region. Thus the ITBs were formed in ion temperature, T_i , and electron temperature, T_e , and electron density, n_e , profiles. These profiles had steep gradients for the ITB layer and reduced gradients for other regions. Figure 1 shows T_i and toroidal rotation velocity of carbon impurity, V_ϕ , profiles measured by charge exchange recombination spectroscopy (CXRS), which were obtained by jogging the plasma, where the plasma was moved inward with 0.1m in 0.1sec during quasi-steady state phase. Steep gradient of T_i was formed around the half of minor radius. However T_i profile became flat in the core region. This profile is a characteristic common with T_e and n_e profiles even for a peaked heating deposition profile [4]. Notched feature in V_ϕ profile was formed near the ITB, which indicates substantial radial electric field shear was formed in the ITB layer. The notched profile frequently appeared in the measured V_ϕ profile of carbon impurity in the reversed shear plasmas with ITB, even for balanced momentum injection. This indicates some nondiffusive processes for toroidal momentum transport. Nondiffusive term for toroidal momentum transport were investigated in JFT-2M tokamak experimentally, This term increases with the increment of T_i gradient and is roughly in inverse proportion to poloidal magnetic field [8]. For more detail explanation using neoclassical treatment, the notch results from parallel heat friction due primarily to the large hydrogenic parallel heat flows driven by large T_i gradient, which drag on the impurity ions in the counter direction [9].

Definitions of ρ_{ITB} , ρ_{foot} and Δ_{ITB} in the ion temperature profile are illustrated in Fig. 1(a). Here ρ_{ITB} and ρ_{foot} are the locations of the ITB center and the ITB foot, and Δ_{ITB} is the ITB width. These values characterize the ITB structures and affect the global confinement property, for example, the large ITB location enhances the confinement property. Figure 2

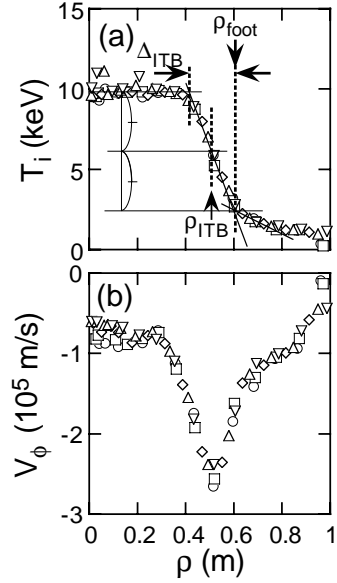


FIG. 1. Profiles of (a) T_i and (b) V_ϕ obtained by jogging the plasma. Different symbols indicate the different timing during the jogging. Definition of the location of the ITB center, ρ_{ITB} , and of the location of the ITB foot, ρ_{foot} , and of the ITB width, Δ_{ITB} .

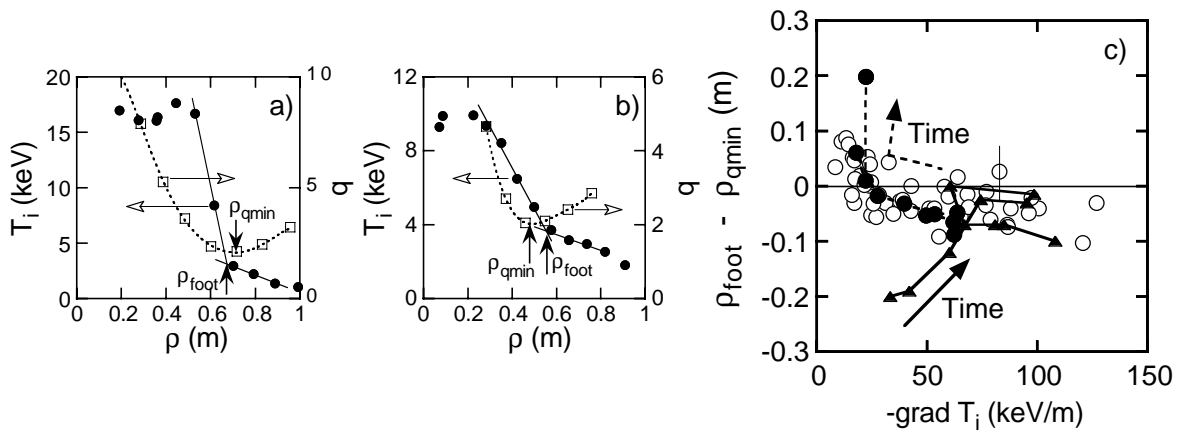


FIG. 2. Profiles of T_i (closed circles) and q (open squares) in the case of (a) steep T_i gradient, (b) reduced T_i gradient. (c) The relation between the T_i gradient and the difference of ρ_{foot} and ρ_{qmin} (open circles) with time traces of the typical high performance discharge (closed triangles) and the ITB degradation discharge (closed circles).

shows T_i and safety factor, q , profiles in the case of (a) the narrow ITB width with steep gradient of T_i and (b) the wide ITB width with reduced gradient of T_i . The ρ_{foot} located inside of the q_{min} position ($\rho_{q_{\text{min}}}$) in the case of (a), while the outside of $\rho_{q_{\text{min}}}$ in the case of (b). Figure 2(c) shows the relation between the T_i gradient at the ITB and the difference of ρ_{foot} and $\rho_{q_{\text{min}}}$ in many discharges (open circles).

The reduced gradient of T_i seems to allow the ITB expansion to outside of $\rho_{q_{\text{min}}}$. The confinement enhancement factor over the L-mode scaling was above 1.4 even in the reduced gradient of T_i . Two time traces are shown in Fig. 2(c). One is in the typical high performance discharge [4], where ρ_{foot} appeared inside $\rho_{q_{\text{min}}}$ with the reduced gradient of T_i firstly, and then moved outward with increasing the T_i gradient. Finally ρ_{foot} located inside $\rho_{q_{\text{min}}}$ (closed triangles with solid line). Another is in the ITB degradation discharge, where ρ_{foot} crossed to $\rho_{q_{\text{min}}}$ with decreasing the T_i gradient, and then ρ_{foot} located outside of $\rho_{q_{\text{min}}}$ (closed circles with dotted line). In this ITB degradation discharge, ρ_{foot} was constant in time, while $\rho_{q_{\text{min}}}$ moved inward due mainly to decreasing the bootstrap current, then ρ_{foot} located outside of $\rho_{q_{\text{min}}}$. In no degradation discharge with steep gradient of T_i , on the other hand, ρ_{foot} followed in the wake of $\rho_{q_{\text{min}}}$ when $\rho_{q_{\text{min}}}$ moved inward. These results indicate that the outward propagation of ITB to the positive shear region across the zero-shear surface is suppressed when T_i gradient is steep. From the viewpoint of the ITB control, in addition, the ITB location with keeping the steep gradient of T_i can be controlled by the external off-axis current drive [10].

It is interesting whether common physics exists in both ETB and ITB. It has been reported that the spatial width of the pedestal of ETB scales with poloidal gyroradius of thermal ions [11,12]. Figure 3(a) shows the relation between Δ_{ITB} and the ion poloidal gyroradius ($\rho_{\text{pi}}^{\text{ITB}}$), where $\rho_{\text{pi}}^{\text{ITB}}$ is evaluated at ρ_{ITB} . Closed circles show the time trace of the typical high performance discharge. The ITB width became narrower with decreasing $\rho_{\text{pi}}^{\text{ITB}}$, where the poloidal magnetic field increased due to the increase of plasma current. This may indicate that the lower boundary of Δ_{ITB} is related to the $\rho_{\text{pi}}^{\text{ITB}}$. In order to examine the parameter dependence of ion poloidal gyroradius ($\sim T_i^{0.5}/B_p$), the lower boundary data is extracted (shade region). Figure 3(b) shows Δ_{ITB} is in inverse proportion to the poloidal magnetic field at the ITB, B_p^{ITB} , for T_i fixed in $\sim 5\text{keV}$ and $\sim 10\text{keV}$. On the other hand, Δ_{ITB} is proportional to square root of T_i for B_p^{ITB} fixed in $\sim 0.24\text{T}$ as shown in Fig. 3(c). Therefore Δ_{ITB} near the lower boundary is proportional to $\rho_{\text{pi}}^{\text{ITB}}$.

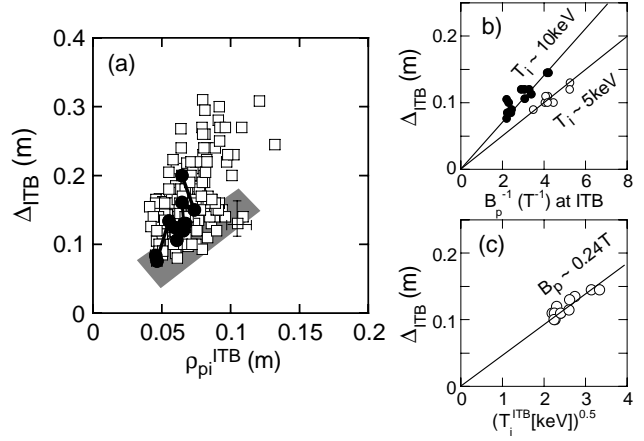


FIG. 3. (a) Δ_{ITB} versus $\rho_{\text{pi}}^{\text{ITB}}$ with the time trace of the typical high performance discharge (closed circles). Shade region indicates the lower boundary. (b) Δ_{ITB} versus B_p^{ITB} for $T_i \sim 5\text{keV}$ (open circles) and $T_i \sim 10\text{keV}$ (closed circles). (c) Δ_{ITB} versus square root of T_i for $B_p^{\text{ITB}} \sim 0.24\text{T}$.

3. Active Control of Pressure Gradient at the Internal Transport Barrier

Active ITB control is one of the most challenging issues in magnetically confined plasmas. For the steady state operation, the active control of ITB strength is indispensable from the viewpoints of transport and stability. Reversed shear plasmas have been achieved high confinement of both particles and heats owing to the ITB formations. MHD instabilities, however, occurred frequently because of steep pressure gradients, and then the discharges were disrupted. Control of pressure gradient is difficult for a fusion reactor where the heating profile is mainly determined by the large alpha heating. In addition, reduction of particle diffusivity and existence of inward convection velocity across the ITB layer led to helium ash accumulation [13]. The helium ash accumulation in the core region during long pulse or steady state operation for a fusion reactor affects the fusion performance due to the dilution of the fuel. Accordingly it is important whether the diffusivity at the ITB can be controlled or not. If the response of diffusivity to stabilizing effect of turbulence is sharp, it is difficult to control the diffusivity level at the ITB without the help of MHD instabilities such as mini-collapses and barrier localized modes. If the response is gradual and/or stepwise, it is beneficial to control the diffusivity [14].

Several theoretical models for transport barrier formation suggest that the ExB flow shear plays an important role in suppressing the level of the turbulence and reducing the correlation length of the turbulence [7]. Therefore there is a possibility that the ITB can be controlled by the modification of the radial electric field profile. The pressure gradient and Lorentz force due to plasma rotation for each ion species balance the radial electric field (E_r) in the toroidal plasma, then

$$E_r = \frac{1}{Z_i e n_i} \frac{dp_i}{dr} + V_\phi B_\theta - V_\theta B_\phi, \quad (1)$$

where Z_i , e , n_i , p_i , V_θ , B_θ and B_ϕ are charge number, electronic charge, ion density, ion pressure, poloidal rotation velocity, poloidal magnetic field and toroidal magnetic field, respectively. The E_r profile is calculated from the profiles of plasma pressure of each species and the measured toroidal rotation velocity of carbon impurity. Since the poloidal rotation is not measurable at the present time, it is estimated on the assumption of neoclassical theory. The procedure to estimate the E_r profile is described in Ref. 15. In general, the E_r profile is mainly determined by V_ϕ profile, because the poloidal rotation is well damped due to parallel viscosity and pressure gradient term is inversely proportional to Z_i . Therefore strong toroidal rotation shear appeared by the notched feature indicates that substantial radial electric field shear is formed near the ITB layer.

Figure 4 shows the trajectories of the injected neutral beams (NBs), which are projected onto the poloidal cross section. JT-60U has eleven units of the positive-ion based neutral beam. Seven units are nearly perpendicular to the plasma current with on- and off-axis deposition, which are useful for the pressure profile control without toroidal momentum injection. The other four units consist of two co-tangential and two counter-tangential NBs with on- and off-axis deposition, which are useful for the control of

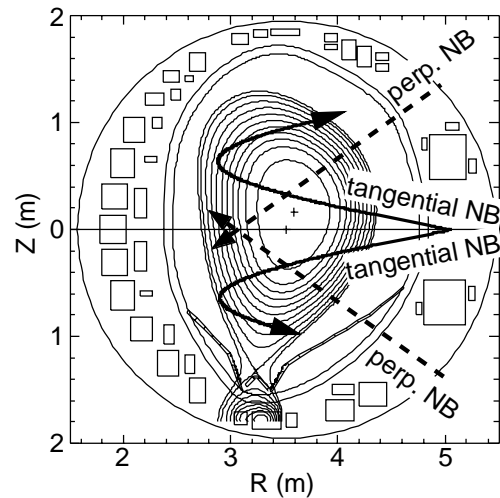


FIG. 4. Poloidal cross section of the analyzed plasmas. The trajectories of tangential NBs (solid curves) and perpendicular NBs (broken curves) are shown.

toroidal rotation and pressure profile. The various combinations of NBs make it possible to modify the E_r profile.

Effects of the toroidal momentum injection by NBs on the core transport properties have been investigated in reversed shear plasmas [15-17]. Figure 5 shows the ion thermal diffusivity, χ_i , profiles in the different directions of toroidal momentum injection, where experimental conditions were toroidal magnetic field of 3.8T, plasma current of 1.5MA and injected NB power of 8MW. These χ_i profiles were obtained by changing the direction of toroidal momentum injection after the ITB formation.

The value of χ_i was decreased to the level of neoclassical value within the narrow region in the balanced (BAL) injection where the injected toroidal momentum was almost canceled. In the unidirectional (CO or CTR) injection, on the other hand, χ_i was higher than that of BAL, while reduced transport region was wider. The level of transport at ITB can be changed by different momentum injection. The dominant term of E_r was different in the balanced or unidirectional injection. Pressure gradient term of the E_r shear (dE_r/dr) was dominant in the BAL, which was formed locally. On the other hand, toroidal rotation term of the E_r shear was dominant in the CO and CTR, which was broader due to the broad deposition profile of momentum source by NB.

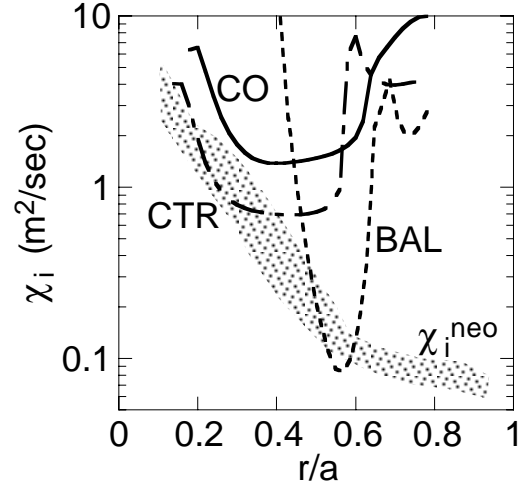


FIG. 5. Ion thermal diffusivity profiles in the different directions of toroidal momentum injection. Shadow region describes neoclassical level.

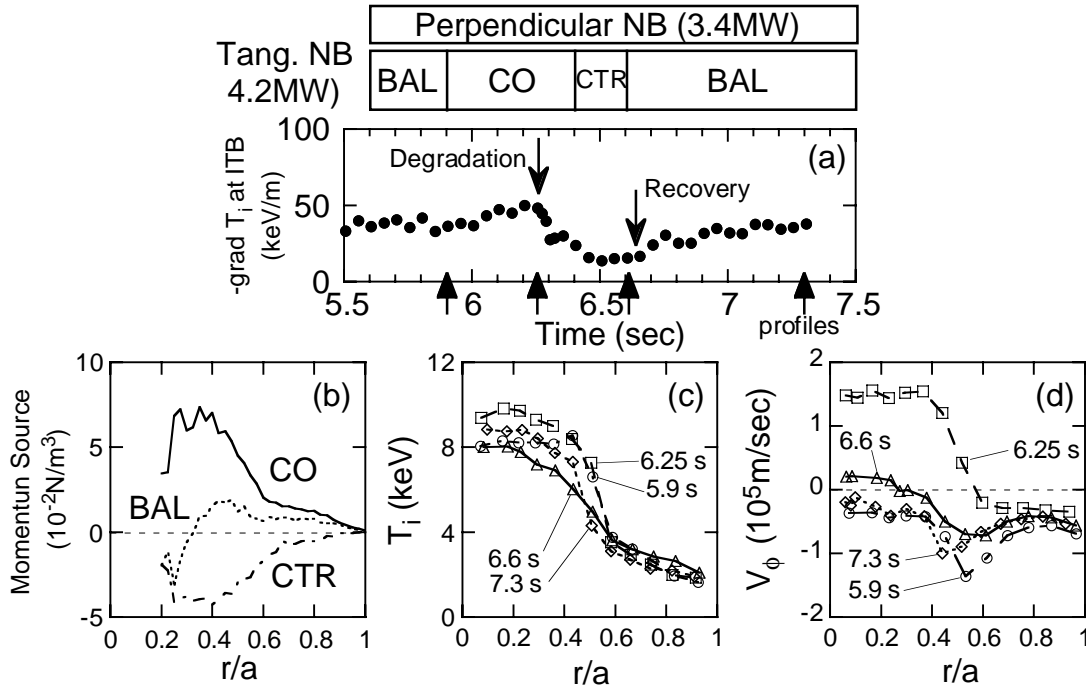


FIG. 6. (a) Time evolution of T_i gradient with the combination of NB. (b) Momentum source profiles in the different directions of toroidal momentum injection. Profiles of (c) ion temperature and (d) toroidal rotation velocity in the active ITB control discharge by changing the direction of toroidal momentum injection.

These experiments were one-way controls, where unidirectional momentum injection caused the degradation of the ITB. The recovery of the ITB is necessary for the active ITB control. Toroidal rotation as well as pressure gradient profile affect the E_r shear profile because E_r is coupled with plasma rotation and pressure gradient in Eq. (1). Since the heating profile can modify the pressure gradient and toroidal momentum injection can modify the toroidal rotation profile, two scenarios are considered demonstrating the active ITB control after the ITB formation. One is control of toroidal rotation; namely changing unidirectional injection to balanced injection for the recovery of ITB. The other is control of pressure gradient; namely the increase of heating power for the recovery of ITB.

Figure 6 shows the demonstration of the active control of ITB strength by changing the direction of toroidal momentum injection. Toroidal magnetic field and plasma current were 3.5T and 1.5MA in this discharge. In quasi-steady state phase after $t=5.6$ sec, the directions of toroidal momentum injection was only changed with the same injected NB power. Up to $t=5.9$ sec, balanced momentum injection used for sustainment of ITB, where two units of tangential NBs and one and half units of perpendicular NBs were injected. Then tangential NBs switched to co-injection up to $t=6.4$ sec. In the co-injection phase, T_i profile was almost the same up to $t=6.25$ sec, while V_ϕ profile changed from notched profile to monotonic one. This was caused by the toroidal momentum source profile, which is calculated by the orbit following Monte Carlo (OFMC) code [18]. The momentum source profile of co-injection has the steep gradient at the ITB layer, which changes V_ϕ profiles from notched to monotonic. The ITB degradation started at $t=6.25$ sec. Ctr-injection was applied during the short period from $t=6.4$ sec to $t=6.6$ sec in order to pull down the plasma rotation. After $t=6.6$ sec, tangential NBs switched to balanced injection. Then ITB growth started even the same injected NB power. As a result, T_i gradient varied from 50keV/m to 15keV/m in spite of no MHD activities.

Figure 7 shows the E_r shear profile and its each component, where poloidal rotation term is smaller than the other terms and is not plotted for simplicity. The change in T_i gradient is strongly related to the change in the V_ϕ term of the E_r shear profile. At the end of the initial BAL phase, pressure gradient, ∇p , term and V_ϕ term added each other, thus the strong E_r shear was formed in the ITB layer. Right before the ITB degradation by co-injection, however, ∇p and V_ϕ terms counterbalanced each other in the outer half region of the ITB layer, while the strong E_r shear remained in the inner half region of the ITB layer. Thus the E_r shear was reduced only in the outer half region of the ITB layer. After this timing, T_i gradient degraded in the whole ITB layer. This result indicates a semi-global nature of the ITB structure [19].

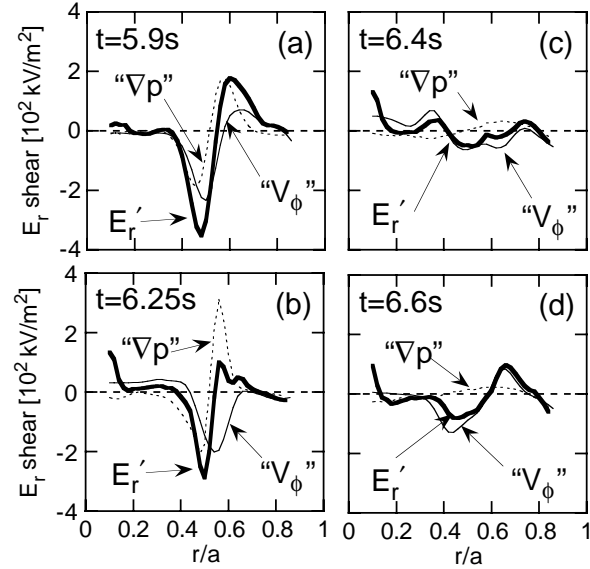


FIG. 7. Profiles of the E_r shear, E_r , and its each component. (a) At the end of the initial balanced injection phase. (b) Right before the ITB degradation by co-injection. (c) During the ITB degradation by co-injection. (d) Right before the ITB recovery by balanced injection.

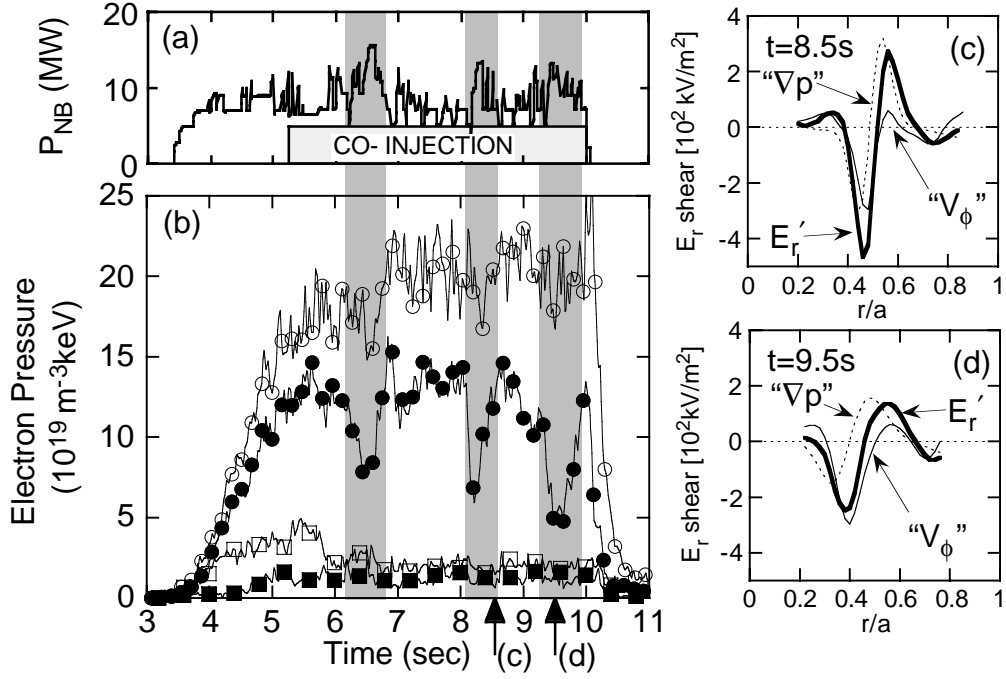


FIG. 8. (a) Waveform of NB power. (b) Time evolution of the electron pressure in each position, normalized radius of 0.3 (open circles) and of 0.5 (closed circles) and of 0.7 (open squares) and of 0.9 (closed squares). Profiles of the E_r shear and its each component (c) at $t=8.5\text{sec}$ (strong ITB phase) and (d) at $t=9.5\text{sec}$ (weak ITB phase).

During the ITB degradation by co-injection the E_r shear became small, where ∇p and V_ϕ terms counterbalanced each other. Right before the ITB recovery by balanced-injection, V_ϕ term grew up and ∇p term was still small. Then E_r shear profile at the end of recovery was similar to the initial BAL phase. The behavior of electron temperature and electron density profile was similar to ion temperature profile. The control of pressure gradient at the ITB was successfully performed by toroidal momentum injection in different directions. The ITB radius after the recovery, however, was slightly smaller than that before the degradation. This is because the ρ_{qmin} moved inward due to decreasing the bootstrap current, as described in Sec. 2. Therefore the external current profile control is necessary for the active ITB control including the ITB location.

The demonstration of the active control of ITB strength by the central heating power during co-injection is shown in Fig. 8. Toroidal magnetic field and plasma current were 3.4T and 0.8MA. The combination of tangential NBs was changed the nearly balanced to the co-dominant injection at $t=5.2\text{sec}$ until the end of the NB heating, where co-NB power of 4.4MW for the ITB degradation, ctr-NB power of 0.75MW for MSE measurement, and perpendicular NB power of 2MW were injected. In this discharge, the feedback control of diamagnetic stored energy with the perpendicular NB power was applied for the active ITB control. Right after the ITB degradation at $t=5.8\text{sec}$, the additional heating power of about 6MW with no toroidal momentum was injected, then the electron pressure at the ITB was recovered by $t=6.9\text{sec}$. Then the ITB was sustained during about 1sec although no additional heating power was injected. The ITB degradation was caused by co-injection as described above. In this

phase, thermal diffusivity was increased, however even then pressure gradient was increased by additional heating power. As a result, self-sustainable E_r shear was formed due to the reduction of the diffusivity, and then ITB was sustained with small heating power. The same behavior was observed after $t=8.2\text{sec}$ and $t=9.0\text{sec}$. The E_r shear was calculated at $t=8.5\text{sec}$ and $t=9.5\text{sec}$, shown in Figs. 8(c) and (d). The E_r shear in the strong ITB phase was larger than that in the weak ITB phase, where the ∇p term changed dominantly.

4. Conclusions

For the purpose of the active ITB control, characteristics of the ITB structure are studied in JT-60U reversed shear plasmas, and then the following results are found. Lower boundary of ITB width is proportional to the ion poloidal gyroradius at the ITB center. Outward propagation of the ITB with steep T_i gradient is limited to $\rho_{q_{\min}}$. However the ITB with reduced T_i gradient can move to the outside of $\rho_{q_{\min}}$. Furthermore the active control of ITB strength based on the modification of the E_r shear profile has been successfully performed by the toroidal momentum injection in different directions or the increase of heating power using NB. The change of E_r shear profile suggests a semi-global nature of the ITB structure.

Acknowledgement

The authors would like to thank the members of JAERI who have contributed to the JT-60U project.

References

- [1] WAGNER, F., et al., Phys. Rev. Lett. 49 (1982) 1408.
- [2] KOIDE, Y., et al., Phys. Rev. Lett. 72 (1994) 3662.
- [3] FUJITA, T., et al., Phys. Rev. Lett. 78 (1997) 2377.
- [4] FUJITA, T., et al., Nucl. Fusion 38 (1998) 207.
- [5] KAMADA, Y., et al., Nucl. Fusion 39 (1999) 1845.
- [6] KIKUCHI, M., Nucl. Fusion 30 (1990) 265.
- [7] BIGLARI, H., et al., Phys. Fluids B 2 (1990) 1.
- [8] IDA, K., et al., J. Phys. Soc. Jpn. 67 (1998) 4089.
- [9] ERNST, D. R., Phys. Plasmas 5 (1998) 665.
- [10] IDE, S., et al., Nucl. Fusion 40 (2000) 445.
- [11] HATAE, T., et al., Plasma Phys. Control. Fusion 40 (1998) 1073.
- [12] GROEBNER, R. J., Phys. Plasmas 5 (1998) 1800.
- [13] TAKENAGA, H., et al., Nucl. Fusion. 39 (1999) 1917.
- [14] KAMADA, Y., Plasma Phys. Control. Fusion 42 (2000) A65.
- [15] SHIRAI, H., et al., Plasma Phys. Control. Fusion 42 (2000) A109.
- [16] SYNAKOWSKI, E. J., et al., Phys. Rev. Lett. 78 (1997) 2972.
- [17] GREENFIELD, C. M., et al., Phys. Plasmas 7 (2000) 1959.
- [18] TANI, K., J. Phys. Soc. Japan 50 (1981) 1726.
- [19] NEUDATCHIN, S. V., et al., IAEA-CN-77/EXP5/01, this conference.